This is an open access article published under a Creative Commons Attribution (CC-BY) License, which permits unrestricted use, distribution and reproduction in any medium, provided the author and source are cited.

ACS AUTHORCHOICE

THE JOURNAL OF PHYSICAL CHEMISTRY A

pubs.acs.org/JPCA Article

Description of Chiral Complexes within Functional-Group Symmetry-Adapted Perturbation Theory—The Case of (S/R)-Carvone with Derivatives of (−)-Menthol

Michał Chojecki, Dorota Rutkowska-Zbik, and Tatiana Korona*

Cite This: J. Phys. Chem. A 2020, 124, 7735−7748 Read Online

ACCESS | Metrics & More | Article Recommendations | Supporting Information

ABSTRACT: Symmetry-adapted perturbation theory (SAPT) and functional-group SAPT (F-SAPT) are applied to examine differences in interaction energies of diastereoisomeric complexes of two chiral molecules of natural origin: (*S*/*R*)-carvone with (−)-menthol. The study is extended by including derivatives of menthol with its hydroxy group exchanged by another functional group, thus examining the substituent effect of the interaction and the interaction differences between diastereoisomers. The partitioning of the interaction energy into functional-group components allows one to explain this phenomenon by the mutual cancellation of attractive and repulsive interactions between functional groups. In some cases, one can identify dominant chiral interactions between groups of atoms of carvone and menthol derivatives, while in many other instances, no major interaction can be distinguished and the net chiral difference results from subtle near cancellation of several smaller terms. Our results indicate that the F-SAPT method can be faithfully utilized for such analyses.

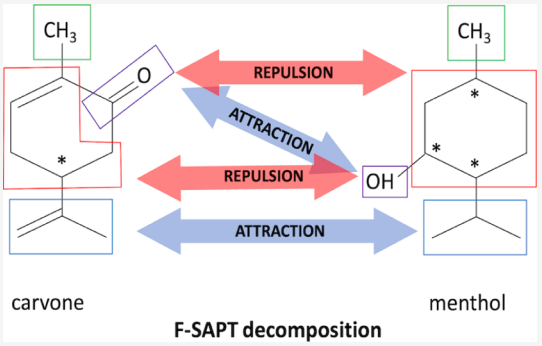

INTRODUCTION

Theoretical prediction of interactions between chiral compounds is still a poorly explored area within the theory of intermolecular forces. In spite of the existence of modern and mature quantum-chemical techniques such as symmetry-adapted perturbation theory (SAPT)[1−3] and its functional-group partitioning (F-SAPT),[4−6] their use for the description of the interactions within complexes composed of chiral molecules is scarce. Recently, we have tested the applicability of these methods on an example of the interaction of three popular chiral drugs: ibuprofen, norepinephrine, and baclofen with building blocks of chiral phases for chromatography: phenethylamine and proline.[7] We also examined the dimers of chlorophyllide and its artificial diastereoisomer with perturbational techniques in ref 8. About the same time, Hemmati and Patkowski applied the same methods for the interaction of propylene oxide complexes.[9] Out of the tested methods, the F-SAPT proved to be the most useful in determining which functional groups are responsible for modulation of the strength of the interaction between chiral molecules. Here, in order to further advance our experience, we decided to study the applicability of F-SAPT for a description of similar noncovalent complexes. As the test case, we selected the (*S*/*R*)-carvone−(−)-menthol pair and its variants in which the menthol hydroxy group is exchanged for another functional group, such as cyano, nitro, halogen, methyl, amino, and so forth. Some of these derivatives can be found in nature, and the synthesis of others was reported in the literature.[10] Such a selection of the model enabled us to examine how minor changes in the structure of the chiral molecule influence its interaction with the chiral partner.

Carvone and menthol constitute one of the main ingredients of essential oils from *Mentha* species,[11] widely used in food and pharmaceutical industries mostly for their smell: (−)-menthol has a spearmint-like smell and (*S*)-(+)-carvone has a caraway-like smell, while the (*R*)-(−)-carvone again has a minty smell. Both serve as popular model molecules of active, natural products, for instance, in studies of interactions with bioreceptors,[12,13] in the formation of conjugates with nanoparticles,[14] in drug-delivery systems,[15] or in odor sensing.[16] Being cheap, abundant, and easily available, menthol is widely used in synthetic chemistry, in particular, in asymmetric synthesis—for extensive reviews, see, for example, refs.[10,17,18] For instance, it was employed as an initiator in an atom transfer radical polymerization of styrene.[19] Similarly, carvone can also serve as a substrate for polymer chemistry.[18,20] (*R*)-Carvone has recently been used to obtain new chiral isoxazoles and pyrazoles having a monoterpenic skeleton, which were further tested for cytotoxicity against human HT-1080, MCF-7, and A-549 cancer cells.[21] (*S*)-Carvone was employed in stereoselective total

Received: July 8, 2020
Revised: August 27, 2020
Published: August 28, 2020

© 2020 American Chemical Society

https://dx.doi.org/10.1021/acs.jpca.0c06266
J. Phys. Chem. A 2020, 124, 7735−7748

synthesis of (−)-daphenylline, an alkaloid present in plants of the *Daphniphyllum* genus, used in Chinese medicine for their curative properties.[22]

Both molecules were subjected to theoretical studies whose aim was mainly to explore the conformational landscape of these naturally occurring species. The conformational studies were carried out both by theoretical methods, mostly Hartree−Fock (HF) and Density Functional Theory (DFT), and compared with the results of experimental vibrational and vibrational circular dichroism spectroscopies.[23−26] Carvone was additionally studied by means of gas electron diffraction supported by theoretical calculations within MP2/6-31G** and DFT:B3LYP/6-31G** methods.[27]

Furthermore, optical rotatory dispersion and circular dichroism of six isomers of (*S*)-(+)-carvone were studied in 17 different solvents and compared with results from calculations for the gas phase with DFT:B3LYP/6-311G(d,p), MP2/6-31(d), CC2, and CCSD methods.[28] (*S*)-Carvone served also as one of the test molecules to compute axial birefringence induced by a magnetic field on the DFT:B3LYP/aug-cc-pVDZ level.[29,30] Because of its applicability in synthetic chemistry, the reactivity of (*R*)-carvone toward peracetic acid in epoxidation and Baeyer−Villiger reactions was explored by employing DFT:B3LYP/6-311G(d,p).[31]

The studies on carvone and/or menthol interactions are so far limited. An interesting study of the chiral recognition of carvone comes from Nandi,[12] who studied chiral sensing of (*R*)- and (*S*)-carvone with dipalmitoylphosphatidylcholine. The system was selected as an in vitro model of chiral recognition of the odorant by lipids.[32] The interaction was studied by the examination of the effective pair potential which is a relatively simple yet effective tool to study the orientation dependence of the intermolecular interactions between chiral species.[33]

The interest in the reactivity of both menthol and carvone and their derivatives results not only from their availability but also from the fact that they bear chiral centers in relatively simple chemical structures. This drove our curiosity to study these molecules as well. In particular, we would like to explore to which extent the F-SAPT can qualitatively and quantitatively predict the strength of the interactions within chiral complexes formed by molecules differing by minor changes in their substituents.

METHODOLOGY

The structures of the complexes under study have been found using a multistep geometry optimization procedure. First, the optimal geometries of carvone and menthol were obtained by performing DFT optimizations starting from structures resulting from the systematic conformer generator.[34] In the second step, these geometries were used as starting points for the geometry optimization of the carvone−menthol or carvone−menthol derivative complexes, where the AutoDock Vina[35] was used to generate starting points for the final DFT optimization. From the resulting minima, the lowest ones were selected for further analysis with SAPT and F-SAPT. The B97-D functional[36] and the aug-cc-pVTZ basis set[37] were utilized for the DFT part of geometry optimizations. The resolution-of-identity procedure, also known as density fitting (DF),[38] was used to approximate two-electron repulsion integrals (ERIs), with the corresponding default auxiliary basis sets.[39] This part of calculations was performed with the TURBOMOLE software package.[40]

The most important quantity for assessing the strength of the intermolecular interactions is the interaction energy, defined as a difference between the electronic energy of the complex AB (*a dimer*) and the sum of energies of the constituent molecules A and B (*monomers*)

$$E_{\mathrm{int}}(\mathrm{AB}) = E(\mathrm{AB}) - (E(\mathrm{A}) + E(\mathrm{B})) \tag{1}$$

where geometries of the monomers are fixed, that is, they are the same in the monomers and the dimer. The interaction energy is a function of relative orientations of the molecules A and B, but in this study, we will focus on the interaction energy calculated at the minimum found from the geometry optimizations of the dimer. The interaction energy for these minimum structures was calculated with SAPT with monomers described at the DFT level[41,42] and with the ERIs treated with DF approximation.[43] The PBE0 functional[44,45] with the Grüning asymptotic correction (AC)[46] was used for the DFT description of the monomers. Vertical ionization potentials (IPs) and the highest occupied molecular orbital (HOMO) energies, needed for the calculation of the AC, were obtained with the PBE0 functional as well. The PBE0AC functional has been found to be among the top performers for various SAPT(DFT) approaches, when compared to the benchmark SAPT(CCSD) method, that is, SAPT with the monomers described on the level of coupled cluster theory truncated after double excitations.[47] The large aug-cc-pVQZ basis set was used[37] for the IPs, while the PBE0 energies of the HOMOs were obtained in the same basis as used in SAPT(DFT). Additionally, the second-order dispersion energy, known to be notoriously difficult to saturate by increasing basis sets, was evaluated by the complete-basis-set (CBS) extrapolation procedure for the correlation energy[48] using the results for aug-cc-pVTZ and aug-cc-pVQZ basis sets in the extrapolation formula. This part of calculations was performed with the Molpro package.[49,50]

The SAPT interaction energy is obtained as a sum of the following components

$$E_{\mathrm{int}}^{\mathrm{SAPT}}(\mathrm{AB}) = E_{\mathrm{elst}}^{(1)} + E_{\mathrm{ind}}^{(2)} + E_{\mathrm{disp}}^{(2)} + E_{\mathrm{exch}}^{(1)} + E_{\mathrm{exch\text{-}ind}}^{(2)} + E_{\mathrm{exch\text{-}disp}}^{(2)} + \delta E_{\mathrm{HF}} \tag{2}$$

The first six terms of the right-hand side of eq 2 have a clear physical interpretation,[51] and the so-called delta HF (δE_{HF}) term estimates selected higher-order contributions.[52] For the unsubstituted case, we also performed an additional analysis of SAPT contributions with monomers described on various Møller−Plesset (MP) levels.[53−58] The latter computations were performed with the Psi4 code[59] in the aug-cc-pVDZ basis set.

The F-SAPT method enables an approximate partitioning of the energy contributions from eq 2. Because the partitioning of the SAPT energy into the intergroup interaction is needed on the semiquantitative level only, we adopted the recipe from ref 5 and utilized the SAPT(HF) and the jun-cc-pVDZ[60] basis in the F-SAPT computations. Because of these differences, the total F-SAPT energies cannot be directly compared to the SAPT(DFT)/CBS results.

In order to facilitate the comparisons between both diastereoisomers, we introduce the difference energy ΔE_{chir} (also called the chirodiastaltic energy[61]), which is defined as

$$\Delta E_{\mathrm{chir}} = E((R)\text{-carvone} - (-)\text{-menthol}) - E((S)\text{-carvone} - (-)\text{-menthol}) \tag{3}$$

for two carvone−menthol complexes and analogously for complexes with derivatives of menthol. Note that this definition is employed for total interaction energies and the partitioned

https://dx.doi.org/10.1021/acs.jpca.0c06266
J. Phys. Chem. A 2020, 124, 7735−7748

Table 1. Components of the SAPT/aug-cc-pVDZ Interaction Energy[a] for Carvone−OH-Menthol Complexes[b] Calculated with Various SAPT Models[c]

	method										
	(DFT)		(HF)		(MP)		(DFT)−(MP)		(DFT)	(HF)	(MP)
	parameter										
component	α	β	α	β	α	β	α	β	chiral discrimination		
$E_{\mathrm{elst}}^{(1)}$	−43.3	−41.3	−43.8	−40.8	−42.5	−40.8	−0.8	−0.4	2.0	3.0	1.7
$E_{\mathrm{exch}}^{(1)}$	70.1	76.7	60.8	68.1	72.8	79.9	−2.6	−3.2	6.6	7.3	7.1
$E_{\mathrm{ind}}^{(2)}$	−27.9	−28.1	−23.0	−23.5	−27.2	−27.5	−0.7	−0.6	−0.2	−0.5	−0.3
$E_{\mathrm{exch\text{-}ind}}^{(2)}$	21.1	22.6	14.9	16.8	17.6	19.7	3.5	2.9	1.5	1.9	2.0
$E_{\mathrm{disp}}^{(2)}$	−58.1	−68.2	−60.3	−72.1	−62.4	−73.6	4.3	5.4	−10.1	−11.8	−11.2
$E_{\mathrm{exch\text{-}disp}}^{(2)}$	7.5	8.9	6.4	7.8	6.4	7.8	1.2	1.2	1.4	1.4	1.4
δE_{HF}	−6.6	−6.3	−6.6	−6.3	−6.6	−6.3	0.0	0.0	0.2	0.2	0.2
$E_{\mathrm{int}}^{\mathrm{TOT}}$	−37.0	−35.7	−51.6	−50.1	−41.8	−40.9	4.8	5.2	1.3	1.5	0.9

[a]Energies are given in kJ/mol. [b]α and β stand for (*S*)-carvone−OH-menthol and (*R*)-carvone−OH-menthol, respectively. [c](X) stands for SAPT(X).

ones. We are also introducing a shorthand description of the (*S*)-carvone−(−)-menthol and (*R*)-carvone−(−)-menthol complexes and denoting them as *S* or *R* complexes, respectively. Moreover, the (−)-menthol and its derivatives are denoted here as X-menthol, where X stands for the −OH group in pristine menthol or the corresponding derivative group.

RESULTS AND DISCUSSION

Comparison of Various SAPT Levels for Carvone−Menthol Interaction. As already mentioned in the Methodology section, the investigation of the stability differences between diastereoisomers formed by the derivative of menthol and (*S*/*R*)-carvone molecules is performed with the SAPT(DFT) method using the asymptotically corrected PBE0 functional (PBE0AC). Although this functional has been already tested in several publications against, for example, CCSD(T) or SAPT(CCSD) benchmarks,[47] it is nonetheless interesting to compare its performance in the present case with respect to other models. To this end, we not only calculated SAPT contributions at the SAPT(HF) level (which is also frequently denoted as SAPT0 and which serves as the base for the F-SAPT model)

$$E_{\mathrm{int}}^{\mathrm{SAPT(HF)}} = E_{\mathrm{elst}}^{(10)} + E_{\mathrm{exch}}^{(10)} + E_{\mathrm{ind,resp}}^{(20)} + E_{\mathrm{exch\text{-}ind,resp}}^{(20)} + E_{\mathrm{disp}}^{(20)} + E_{\mathrm{exch\text{-}disp}}^{(20)} + \delta_{\mathrm{HF}}^{(2)} \quad (4)$$

but also beyond this model to show the importance of the intramonomer electron correlation for energy components in SAPT where monomers are described on various levels of the MP theory, according to the methodology developed by Moszyński et al.[62−66]

$$E_{\mathrm{int}}^{\mathrm{SAPT2+}} = E_{\mathrm{int}}^{\mathrm{SAPT(HF)}} + E_{\mathrm{elst,resp}}^{(12)} + E_{\mathrm{exch}}^{(11)} + E_{\mathrm{exch}}^{(12)} + {}^{t}E_{\mathrm{ind}}^{(22)} + {}^{t}E_{\mathrm{exch\text{-}ind}}^{(22)} + E_{\mathrm{disp}}^{(21)} + E_{\mathrm{disp}}^{(22)} \quad (5)$$

and including the third order of the intermolecular interaction

$$E_{\mathrm{int}}^{\mathrm{SAPT2+3}} = E_{\mathrm{int}}^{\mathrm{SAPT2+}} + E_{\mathrm{elst,resp}}^{(13)} + E_{\mathrm{disp}}^{(30)} + E_{\mathrm{exch\text{-}ind}}^{(30)} + E_{\mathrm{ind,resp}}^{(30)} + E_{\mathrm{exch\text{-}disp}}^{(30)} + E_{\mathrm{ind\text{-}disp}}^{(30)} + E_{\mathrm{exch\text{-}ind\text{-}disp}}^{(30)} - \delta_{\mathrm{HF}}^{(2)} + \delta_{\mathrm{HF}}^{(3)} \quad (6)$$

The computations of these corrections were performed in a somewhat smaller aug-cc-pVDZ basis set because of high computational costs of some of them. Table 1 shows SAPT components for the SAPT(DFT) with the PBE0AC functional, SAPT(HF), and SAPT2+ methods, abbreviated as (DFT), (HF), and (MP), respectively, in this table, followed by differences between the energy components obtained by SAPT(DFT) and SAPT2+ and, finally, the chiral discrimination for individual SAPT components, as reproduced by all three variants of SAPT methods. For the SAPT(MP) method, the electrostatic term is reproduced up to the third order in terms of the intramonomer fluctuation operator *W*, the first-order exchange, second-order induction and exchange induction, and second-order dispersion, to the second *W* order, while the small exchange-dispersion term is kept on the SAPT(HF) level. The values of individual corrections listed in eqs 4−6 are additionally listed in Table S1 in the Supporting Information.

First of all, the comparison of SAPT(HF) and two remaining models shows that the lack of intramonomer electron correlation introduces errors of the order of 10 kJ/mol in the total interaction energies and $E_{\mathrm{exch}}^{(1)}$ components and of about 5 kJ/mol for induction and exchange-induction terms. Strangely enough, the discrepancies for the dispersion energy are much smaller, while it is known that dispersion is a purely electron-correlation component of the interaction energy. However, a more detailed analysis of the correlation corrections to dispersion reveals that this small discrepancy results from a near cancellation of two terms, which are formally of a different order in terms of the intramonomer fluctuation operator: the $E_{\mathrm{disp}}^{(21)}$ terms are positive and large (10 and 13 kJ/mol for *S* and *R* diastereoisomers, respectively), while the $E_{\mathrm{disp}}^{(22)}$ is negative and equal to −12 and −14 kJ/mol, respectively (see Table S1).

Compared to large differences between SAPT(HF) and SAPT(MP), the SAPT(DFT) and SAPT(MP) components are quite close to each other. The highest relative differences occur for both second-order exchange terms, which can be anticipated, because the exchange-dispersion term within SAPT(MP) is calculated without any intramonomer correlation included, while the second-order exchange-induction intramonomer correlation contribution ${}^{t}E_{\mathrm{exch\text{-}ind}}^{(22)}$ is estimated from the ratio of ${}^{t}E_{\mathrm{ind}}^{(22)}/E_{\mathrm{ind,resp}}^{(20)}$. It has been already noted in ref 67 that this ratio gives poor estimates of the intramonomer correlation in many cases in comparison to the benchmark SAPT(CCSD) results. In terms of absolute differences between SAPT(DFT) and SAPT2+, it is the dispersion, the second-order exchange induction, and the first-order exchange components which

https://dx.doi.org/10.1021/acs.jpca.0c06266
J. Phys. Chem. A 2020, 124, 7735−7748

show the largest discrepancies. However, the differences in total interaction energies are smaller because these discrepancies partially cancel each other.

Finally, because the main goal of the present study is the examination of the chiral discrimination between two diastereoisomers, it is interesting to see whether all three SAPT models give the ΔE_{chir} values of the same sign and similar magnitude for all SAPT components. The last three columns of Table 1 show that this is indeed the case. In particular, the largest, the near-zero, and the smallest ΔE_{chir}'s are faithfully reproduced (see the values for $E^{(1)}_{exch}$, $E^{(2)}_{ind}$, and $E^{(2)}_{disp}$, respectively), in spite of the fact that the intramonomer correlation plays the important role in the first two terms. Therefore, the most primitive SAPT(HF) model, utilized within F-SAPT partitioning, seems to be a safe choice for a difference analysis of the interaction energy components for diastereoisomers involving (*S*)- or (*R*)-carvone and menthol derivatives. It should be noted that the $|\Delta E_{chir}|$ for the third-order polarization and exchange SAPT components do not exceed 3 kJ/mol and are of the opposite sign for the component and its exchange counterpart, so altogether they do not play any significant role in chiral discrimination.

Performance of SAPT(DFT) Interaction Energies. The lowest energy conformers for diastereoisomeric complexes are drawn in Figure 1. Additionally, the Cartesian coordinates for these complexes are listed in the Supporting Information.

The SAPT(DFT) interaction energies and their decomposition, according to eq 2, are presented in Table 2. As noted in the Methodology section, the basis set dependence of the dispersion contribution known from many previous studies[68] requires the usage of the CBS estimation for this term, while other SAPT components are already well saturated in the aug-cc-pVQZ basis; therefore, no CBS procedure is necessary for these energies (see Tables S2−S5 in the Supporting Information).

All studied complexes have quite high absolute values of interaction energy, which depend on the substituent type. The strongest attraction occurs for the complexes of carvone with COOH-menthol and the weakest occurs for with CH_3-menthol, while the unsubstituted OH-menthol case represents the second strongest attraction among all studied systems. The attraction of the carvone−COOH-menthol complexes result not only from the electrostatics, dispersion, and net induction ($E^{(2)}_{ind} + E^{(2)}_{exch\text{-}ind}$) but also from larger contribution of δE_{HF}. The replacement of the −OH group by its heavier analogue (−SH) leads to a further weakening of the interaction. The examination of the SAPT components shows that this weakening results from the decrease in absolute values of the electrostatics and induction terms, while the dispersion contribution remains less affected by the substituent change. This finding can be explained by the assumption that this interaction is dominated by the H-bond, which becomes weaker for sulfur replacing oxygen. Starting from the −SH substituent, the interaction energies of the remaining cases are in a range differing by at most 5 kJ/mol. Unexpectedly, the halogen series (−F, −Cl, or −Br substituents) does not show large differentiation of the interaction energy either.

The flattening of the interaction energies means that also the chiral differences are small. For the case with the strongest attraction (carvone−COOH-menthol), the ΔE_{chir} amounts to only 2 kJ/mol, while the two largest absolute values of ΔE_{chir} occur for the carvone−CN-menthol and carvone−NO_2-menthol complexes (−4.8 and −4.6 kJ/mol, respectively). This chiral differentiation is still almost four times larger than

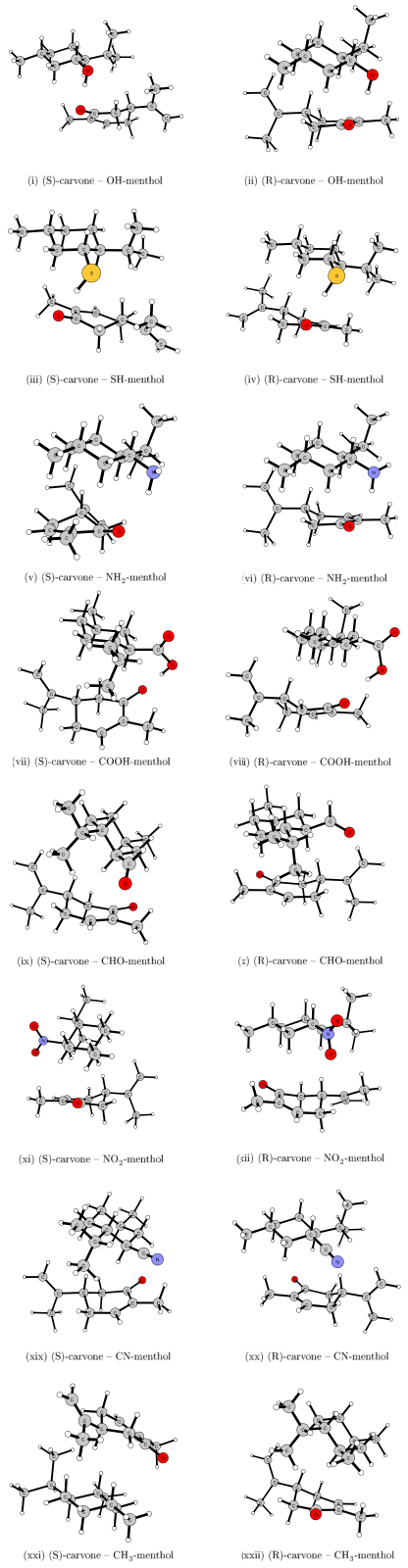

Figure 1. Optimized structures of the complexes under study.

that for the original carvone−OH-menthol complex (1.2 kJ/mol). Therefore, the functionalization of the menthol can, in principle, lead to a better chiral recognition, although these differences are still quite small for all studied cases.

Note that although for almost all complexes, the constituent molecules are polar, the total first-order contribution is always

https://dx.doi.org/10.1021/acs.jpca.0c06266
J. Phys. Chem. A 2020, 124, 7735−7748

Table 2. Components of the SAPT Interaction Energy for the Complexes under Study in the CBS Limit[a,b,c]

complex	$E^{(1)}_{elst}$	$E^{(1)}_{exch}$	$E^{(2)}_{ind}$	$E^{(2)}_{exch\text{-}ind}$	$E^{(2)}_{disp}$	$E^{(2)}_{exch\text{-}disp}$	δE_{HF}	E^{SAPT}_{int}	δE_{chir}
(*S*)-carvone−OH-menthol	−43.3	70.1	−27.9	21.1	−59.8	7.7	−6.6	−38.6	1.2
(*R*)-carvone−OH-menthol	−41.3	76.6	−28.1	22.5	−70.0	9.1	−6.3	−37.4	
(*S*)-carvone−SH-menthol	−29.1	65.0	−20.9	17.4	−67.4	8.2	−5.3	−32.1	3.5
(*R*)-carvone−SH-menthol	−26.8	66.1	−19.5	15.8	−66.7	8.0	−5.6	−28.7	
(*S*)-carvone−NH_2-menthol	−27.3	62.5	−19.4	16.3	−66.5	8.0	−4.3	−30.7	2.6
(*R*)-carvone−NH_2-menthol	−27.6	68.1	−22.3	19.1	−69.3	8.7	−4.8	−28.1	
(*S*)-carvone−COOH-menthol	−63.2	102.6	−41.9	29.0	−78.1	10.3	−11.1	−52.5	2.0
(*R*)-carvone−COOH-menthol	−61.8	101.3	−41.6	30.1	−78.8	10.7	−10.4	−50.5	
(*S*)-carvone−CHO-menthol	−20.2	54.8	−15.3	12.1	−63.6	6.8	−3.6	−28.9	2.8
(*R*)-carvone−CHO-menthol	−17.6	50.3	−14.5	12.1	−59.5	6.5	−3.3	−26.1	
(*S*)-carvone−NO_2-menthol	−19.4	53.7	−15.0	11.7	−63.2	6.6	−3.6	−29.2	−4.6
(*R*)-carvone−NO_2-menthol	−29.4	60.2	−18.8	14.4	−62.0	7.1	−5.2	−33.7	
(*S*)-carvone−F-menthol	−23.2	53.1	−17.5	14.2	−57.8	6.7	−4.0	−28.5	1.0
(*R*)-carvone−F-menthol	−22.5	55.8	−17.0	14.1	−61.2	7.1	−3.6	−27.5	
(*S*)-carvone−Cl-menthol	−19.9	53.7	−14.1	11.7	−60.3	6.5	−3.8	−26.1	−3.6
(*R*)-carvone−Cl-menthol	−21.7	54.2	−16.6	14.0	−62.9	7.0	−3.8	−29.7	
(*S*)-carvone−Br-menthol	−25.6	60.3	−24.0	21.1	−67.2	8.1	−4.3	−31.6	−0.5
(*R*)-carvone−Br-menthol	−24.8	59.5	−21.0	18.1	−67.6	8.0	−4.3	−32.1	
(*S*)-carvone−CN-menthol	−20.6	55.8	−15.2	11.8	−63.6	6.8	−3.6	−28.6	−4.8
(*R*)-carvone−CN-menthol	−23.7	54.9	−16.4	12.6	−63.7	6.9	−4.0	−33.4	
(*S*)-carvone−CH_3-menthol	−17.4	52.7	−13.0	11.1	−62.4	6.7	−3.3	−25.6	0.9
(*R*)-carvone−CH_3-menthol	−16.2	51.1	−13.1	11.3	−61.1	6.6	−3.4	−24.8	

[a]Energies are given in kJ/mol. [b]The last column shows the energy differences for the second and first diastereoisomers, as defined in eq 3. [c]Extrapolation from the aug-cc-pVTZ and aug-cc-pVQZ basis sets.

strongly repulsive, and the major attractive contribution is the second-order dispersion. The differences between dispersion terms are, however, much smaller than differences between electrostatics and first-order exchange contribution; therefore, the latter terms contribute the most to the interaction energy differences between complexes with various derivatives of menthol.

Partitioning of the Interaction Energy with F-SAPT. For the purpose of F-SAPT partitioning, both monomers are divided into several parts of various chemical characters (see Figure 2, in which all the chiral carbons are additionally marked

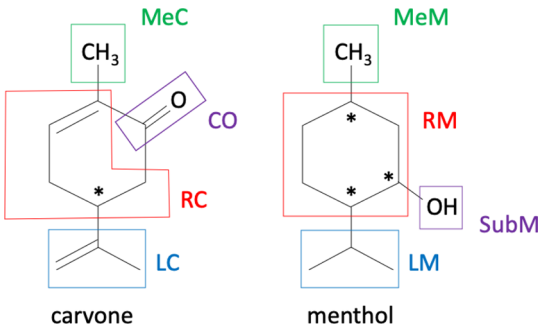

Figure 2. Partition of the considered monomers used in the F-SAPT analysis.

with asterisks). For the carvone molecule, we first distinguish the ring (which is composed of all atoms forming the cyclohexene ring with the exception of the carbon atom forming the carbonyl group). In some cases, it will be useful to further divide this ring into the part containing the double bond and the remaining chain of three C atoms. The remaining groups of carvone are the carbonyl group itself (−CO), the short $-CH_3$ moiety, in the following denoted as MeC, and a longer aliphatic group (−C═CH_2CH_3), denoted here as LC. The only chiral center of carvone is the carbon atom to which the LC group is attached. Therefore, according to the three-point rule, the interactions involving LC or the ring can be considered as potentially chirally discriminating.

For the menthol molecule, we distinguish the cyclohexane ring, the −OH group (which is replaced by other functional groups in the further part of the study), the short $-CH_3$ moiety, denoted as MeM, and a longer aliphatic group (−$CHCH_3CH_3$), denoted here as LM. There are three chiral centers in the menthol molecule. These are the carbon atoms from the menthol ring to which cyclohexane substituents (MeM, −OH, and LM) are attached. As a consequence, chiral discrimination might result from the interactions of all fragments of menthol.

The F-SAPT energy terms (electrostatics, induction, etc.) partitioned into components attributed to pairwise interactions of atomic groups belonging to the carvone and modified menthol molecules are presented in a graphical form in the Supporting Information. In the following sections, we will discuss the most important interaction types between these groups, that is, those which contribute the most to the total interaction energy or to the chiral discrimination. The importance of the F-SAPT contributions resulting from the interaction between these functional groups is schematically depicted in Figure 3.

Carvone−Menthol Complexes. We begin our discussion with the "parent" complex interaction of (*S*)- or (*R*)-carvone with an unsubstituted menthol molecule. The inspection of the geometry patterns of the lowest conformers for these two diastereoisomers allows us to distinguish structural motifs which are present in the majority of studied complexes, that is, (i) hydrogen bonds (possibly also nonstandard ones), (ii) ring−ring interactions, and (iii) interactions between side aliphatic groups (MeC···MeM, LC···LM, MeC···LM, and LC···MeM).

Both carvone−menthol complexes are formed in such a way that a H-bond between −CO and −OH groups is developed.

https://dx.doi.org/10.1021/acs.jpca.0c06266
J. Phys. Chem. A 2020, 124, 7735−7748

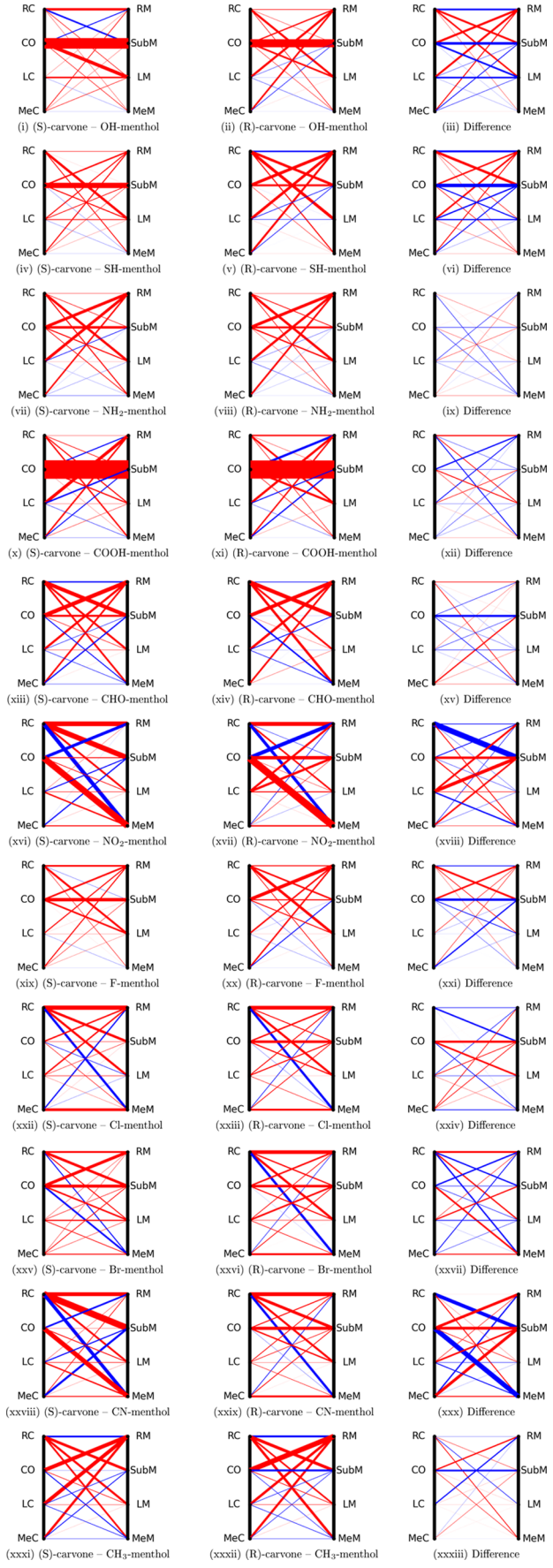

Figure 3. Interaction graphs for the complexes under study. Carvone and the derivative of menthol (depicted as black vertical lines) each are divided into four fragments, as described in the main text, and are abbreviated as RC (ring), CO (carboxylic group), LC (long side-group), and MeC (methyl) for carvone and RM (ring), SubM (OH or substituent), LM (long side-group), and MeM (methyl) for menthol or the derivative of menthol. The red and blue lines depict attractive and repulsive contributions from the F-SAPT study, respectively, while the line thickness is proportional to the absolute value of the interaction energy. The rightmost figure shows differences in F-SAPT energies between the *R* and *S* diastereoisomers.

The importance of this bond for the total interaction can be seen from the corresponding graphs (see Figure 3i,ii) and from values of the total F-SAPT interaction energies between these two groups, which are equal to −32 and −25 kJ/mol for (*S*)-carvone−OH-menthol and (*R*)-carvone−OH-menthol, respectively. The partitioning of these energies into SAPT components shows features of the typical H-bond, that is, a low electrostatic energy which is only partially damped by exchange interaction, accompanied with a net induction contribution, which is, however, of a secondary importance. The geometric features of the O···H−O moiety are also characteristic for the H-bond. First of all, the intermolecular O···H distance is equal to 2.00 and 2.13 Å for the *S* and *R* cases, respectively, which confirms a stronger attractive contribution from F-SAPT for the former case. The O−H bonds in the hydroxyl groups are elongated in comparison to the isolated menthol, and the increase in bond length is again larger for the *S* case, in agreement with the stronger character of the H-bond in this complex (the corresponding lengths denote 0.967, 0.970, and 0.973 Å for isolated menthol and menthol in *R* and *S* complexes, respectively). The O···H−O angle differs from an optimal value of 180° by 19 and 17°, respectively, for the (*S*)-carvone−OH-menthol and (*R*)-carvone−OH-menthol cases. The reason why the O···H−O angle is smaller than 180° is the fact that the rest of menthol moiety would be then farther apart from carvone, thus making the attractive van der Waals interaction between other fragments smaller. For instance, the bending of the H-bond makes it possible to increase the dispersion contribution in the interaction of the carvone ring with LM or the menthol ring. The dispersion contribution is the lowest for the ring−ring interaction for the (*R*)-carvone−OH-menthol complex, where it amounts to as much as −18 kJ/mol. It does not count as one of the strongest interactions only because of the large first-order repulsive exchange term, which almost cancels the attractive dispersion contribution. Another example of large attractive contributions is the mainly electrostatic interaction between the carboxyl group and LM, which is especially pronounced for the (*S*)-carvone−OH-menthol case (−11 kJ/mol). As can be seen from the graphs, there are several secondary interactions which should be considered in order to obtain the full interaction pattern of carvone with menthol. For the (*S*)-carvone−OH-menthol case, the absolute value of the interaction energy is above 4 kJ/mol for the following interactions: three attractive interactions, that is, between the CO group and LM, LC, and LM, and between both rings, and the repulsive interaction between the carvone ring and the −OH group. From these interactions, only the first one (−CO with LM) is above the 4 kJ/mol threshold for the (*R*)-carvone−OH-menthol complex. However, there are other secondary attractive contributions in the latter case, resulting from the interaction of the carvone ring with LM, LC, or MeC with the menthol ring.

https://dx.doi.org/10.1021/acs.jpca.0c06266
J. Phys. Chem. A 2020, 124, 7735−7748

Because the total ΔE_{chir} for the complex of carvone with menthol is very small (ca. 1 kJ/mol) in spite of a significant ΔE_{chir} value for the O−H···O═C interaction (+8 kJ/mol), it is interesting to also examine the interaction energy differences between the *R* and *S* diastereoisomers (see Figure 3iii). The graph shows that the dominance of the H-bond, seen for graphs (depicting total interaction energies for the *S* and *R* isomers), disappears in the ΔE_{chir} graph. Apart from the H-bond contribution, one can point to several more interaction energy differences of similar weight and of opposite signs. A qualitative analysis of the main (i.e., thick) interaction lines for the carvone group gives one negative and two positive contributions for the CO group, one positive and two negative contributions for the ring, and one positive and one negative contribution for LC, thus suggesting the approximate cancellation of positive and negative ΔE_{chir} terms. The explicit addition of these terms shows that indeed the net contribution of the −CO group to the total ΔE_{chir} is positive, of the carvone ring is negative, and of LC is close to zero, which leaves us with an insignificant total ΔE_{chir} = 1 kJ/mol. Therefore, the chiral discrimination of the (*S*)-carvone−OH-menthol and (*R*)-carvone−OH-menthol complexes is hardly possible in spite of the presence of several interactions which individually are chirally discriminating. Accidentally, a quantitative agreement between SAPT(DFT)/CBS interaction energy differences and F-SAPT (i.e., SAPT0/jun-cc-pVDZ) interaction energies is observed for the menthol−carvone pair of complexes.

By exchanging the −OH group of menthol for other popular functional groups, 22 complexes were generated, which will be reviewed below. The complexes are discussed starting from those possessing the typical H-bond and followed by the remaining cases.

Carvone−SH-Menthol Complexes. Let us first discuss the analogue of menthol, in which the −OH group is replaced by the heavier −SH one (see Figure 3iv−vi), resulting in 5-methyl-2-(propan-2-yl)cyclohexane-1-thiol or menthylmercaptan. Menthylmercaptan turns out to have a flavor of a grapefruit.[69] For notation consistency, we will denote menthylmercaptan as SH-menthol in the rest of this paper.

Similarly, as for the complexes formed by menthol, the quantitative agreement between total SAPT interaction energy differences (ΔE_{chir}) and the F-SAPT interaction energies is detected: the chiral discrimination of SH-menthol is about three times larger than that found for menthol and amounts to about 3.5 kJ/mol, according to SAPT(DFT) (see Table 2), with the (*S*)-carvone−SH-menthol more stable than (*R*)-carvone−SH-menthol. For the (*S*)-carvone−SH-menthol complex, stabilization comes predominantly from the interaction of the −SH and −CO groups, as can be expected in view of the H-bond creation. However, this interaction is weaker than that in the unsubstituted menthol, so other interactions between functional groups play a more important role in this case. The second most important interaction occurs between the carvone ring and the LM group. For the (*R*)-carvone−SH-menthol complex, the SH···O═C interaction is even weaker, and it is of the same importance as the −SH group attraction to the carvone ring. There are more interacting pairs which are energetically quite close to the weakened H-bond, such as −CO with the menthyl ring and the carvone ring or LC with −SH; therefore, one cannot name a clear leader in this case. Another interesting feature is a comparably strong dispersion interaction between the rings for the (*R*)-carvone−SH-menthol case, which is however completely canceled by the valence repulsion (exchange), so the net ring−ring interaction is weakly repulsive.

Surprisingly, geometrical parameters suggest a stronger H-bond for the (*R*)-carvone−SH-menthol derivative (the O···H bond length is equal to 2.29 Å, and the S−H···O angle is 176.5°, which should be compared with the values 2.35 Å and 160°, respectively, for the second diastereoisomer). As noted above, the opposite situation is encountered according to the F-SAPT analysis—the S−H···O═C interaction energies are equal to −17 and −6 kJ/mol for the *S* and *R* cases, respectively. All components of this energy are similar to one another in both complexes except for electrostatics, which is more attractive by −10 kJ/mol for (*S*)-carvone−SH-menthol. The analysis of the interaction of unperturbed charges could lead us to a plausible explanation of this peculiar phenomenon. First of all, one should emphasize that F-SAPT interaction energy envelops also the interaction with the carbon atom from the carboxyl group (unfortunately, the limitations of the F-SAPT procedure do not allow us to extract just single oxygen atom as a fragment); therefore, this atom may in some cases suppress the attractive H-bond. In the present case, the S···C distance is about 0.28 Å longer in the (*R*)-carvone−SH-menthol case, so the attraction of the carbon and sulfur atoms, bearing a partial positive and negative charge, respectively, is stronger for the (*S*)-carvone−SH-menthol diastereoisomer. Apparently, the weight of the O···H−S and C···H−S interactions results in the higher attraction of the whole carboxyl group for the (*S*)-carvone−OH-menthol in spite of the more frustrated and longer H-bond.

Because tthe −SH and −OH groups have similar properties, it will be illustrative to compare interaction properties for both pairs of diastereoisomers. From comparison of geometries of both *S*- and *R*-type complexes, one can see that many pairs of groups are in a similar position to each other for the menthol and SH-menthol complex. The comparison of the SAPT components for these pairs reveals that the induction and dispersion components are, in many cases, very similar for carvone−menthol and carvone−SH-menthol complexes. On the other hand, only a subset of these pairs shows no significant difference for the case of the electrostatic contribution, which can be explained by the known larger anisotropy of the latter term. It means that a small disturbance in relative positions of the groups may result in a different electrostatic term, while other contributions are not so sensitive to this geometry factor. Among pairs which have practically the same interaction energies and all the components, one can name the carvone ring, LC or MeC interacting with MeM for the (*S*)-carvone case, and −CO, LC, or MeC interacting with LM for the (*R*)-carvone. In other cases, such as, for example, LC or −CO interacting with LM (the *S* case) or with MeM (the *R* case), the SAPT components are similar with the exception of the electrostatic term, which can differ by 2.4 up to 13 kJ/mol between the *R* and *S* cases, depending on the interacting pair.

Carvone−NH_2-Menthol Complexes. For the complex of carvone with NH_2-menthol (menthyl amine), one expects the main stabilization from the H-bond formed between the amino group of the menthol derivative and the −CO group of carvone. Indeed, in both complexes, one observes the H-bond between these two groups, but it is surprisingly weak, as can be judged from both the geometry parameters and the F-SAPT interaction energy. For the (*S*)-carvone−NH_2-menthol and (*R*)-carvone−NH_2-menthol cases, the O···H distances are equal to 2.47 and 2.42 Å, respectively, and the N−H···O angles are equal to 157 and 155°, respectively, while the F-SAPT interaction energy

https://dx.doi.org/10.1021/acs.jpca.0c06266
J. Phys. Chem. A 2020, 124, 7735−7748

between the −CO and amino groups equal −8 and −6 kJ/mol, respectively. It should be noted that the absolute values of these energies are four times smaller than those for the (*S*)-carvone−OH-menthol and (*R*)-carvone−OH-menthol complexes. The graphs (see Figure 3vii,viii) show that there are three more attractive interactions of a similar magnitude for the present case, in a sharp contrast to the −OH and −SH substituents. These additional interactions occur between the −CO or LC group and the menthol ring and between the carvone ring and the LM group. It is interesting to see that among all interaction components, the most important contribution is the dispersion between both rings (−22 and −20 kJ/mol for *S* and *R* complexes, respectively). However, this attractive component is almost completely canceled by the first-order exchange contribution, which is why the total ring−ring interaction is small (−1 kJ/mol for both cases).

Overall, the chiral discrimination for both diastereoisomers is relatively small and equals 2.6 kJ/mol, according to both SAPT(DFT) and F-SAPT. The absolute values of all ΔE_{chir} contributions are small (see Figure 3ix), and one cannot distinguish any particular components, which contribute to chiral discrimination.

Carvone−COOH-Menthol Complexes. The next pair of complexes under study are diastereoisomers between (*S*)- or (*R*)-carvone and (1*S*,2*R*,5*S*)-2-isopropyl-5-methylcyclohexane-carboxylic acid (denoted here as COOH-menthol). Two graphs corresponding to these complexes (see Figure 3x,xi) are dominated by the strong attraction between the −CO and −COOH groups, which according to the F-SAPT partitioning amounts to −57 and −56 kJ/mol for (*S*)-carvone−COOH-menthol and (*R*)-carvone−COOH-menthol, respectively. This attractive contribution results from the H-bond developed between the oxygen of the carbonyl group from carvone and −OH from the carboxylic group of the menthol derivative. Also, the geometry features confirm the existence of the strong H-bond: the O···H distance is quite short as for the intermolecular bonding (1.83 and 1.89 Å for the *S* and *R* cases, respectively). In the case of (*S*)-carvone−COOH-menthol, the O···H−O angle is close to an optimal value of 180° (177°), while for the (*R*)-carvone−COOH-menthol complex, it is 10° smaller. The more detailed examination of SAPT components of these interaction energies reveals a typical pattern for the H-bond, that is, very low electrostatic interaction (−61 and −57 kJ/mol for the *S* and *R* cases, respectively) only partially damped by the first-order exchange contributions and significant net induction interaction (−16 and −14 kJ/mol, respectively). The second strongest contribution comes from the interaction of LC with the ring of the menthol derivative; however, it is much weaker (−10 and −7 kJ/mol for the *S* and *R* complexes, respectively). Although the difference of the interaction energies between the −CO and −COOH groups corresponds to the total ΔE_{chir} (both are equal to 1 kJ/mol), this similarity is accidental. The inspection of the graphs depicting ΔE_{chir}'s for the F-SAPT partitioning (see Figure 3xii) reveals that there exist more pronounced differences in interactions between two groups, such as the ring−ring interaction (ΔE_{chir} = −4 kJ/mol) or −CO interacting with the menthol derivative ring (ΔE_{chir} = +4 kJ/mol) and several others. However, many of these differences are of the opposite sign, and they cancel each other to a large extent, leaving a small total ΔE_{chir} value.

Carvone−CHO-Menthol Complexes. In the complexes of carvone with CHO-menthol and the remaining complexes under study, there is no typical H-bond, which, in all previous cases, played the major role in the effective binding of both molecules. The lack of this strong "anchoring" contact point of the monomers can result in a different relative orientation of carvone and the derivative of menthol, as compared to the H-bonded complexes discussed above. This happens also for the case of carvone−CHO-menthol diastereoisomers, where both carbonyl groups are situated roughly on the opposite sides of the complex. The analysis of F-SAPT graphs (see Figure 3xiii,xiv) shows two equally important interactions: between the ring of carvone and the −CHO group and between the −CO from carvone and the ring of the menthol derivative. The first of these two interactions has an interaction energy of −12 kJ/mol for both diastereoisomers, while the second has interaction energies of −12 and −11 kJ/mol for (*S*)-carvone−CHO-menthol and (*R*)-carvone−CHO-menthol cases, respectively. Although the first interaction energy is identical for the *S* and *R* complexes, it is composed of a different mix of components. In both complexes, the electrostatics plays the most important attractive role (−8 and −9 kJ/mol, respectively), but because of the larger separation of the −CHO group and the carvone ring for the *R* case, there is almost no exchange contribution, while for the *S* complex, it does affect the interaction to some extent (2 kJ/mol). On the other hand, the smaller distance results in a higher dispersion contributions (−5 vs −2 kJ/mol for the *S* and *R* cases), so altogether, the total interaction energy is the same in both cases. The nature of the second most important interaction is more typical for closer-lying groups: the interaction energy is composed of three contributions of a similar weight (attractive electrostatics and dispersion and repulsive exchange). The most important chirally discriminating interactions come from the −CHO group. One is the attractive interaction with −CO (−6 kJ/mol) of the pure electrostatic character for the (*S*)-carvone−CHO-menthol, while it is equal to 0 kJ/mol for (*R*)-carvone−CHO-menthol. This is in line with the observed geometry of both systems because (i) both groups are polar and far apart from each other and (ii) the distance between groups (measured as distance between their oxygen atoms) is larger in the second case (7.12 Å vs 5.24 Å). The second most important chirally discriminating interaction between MeC and −CHO is also of a similar type, that is, the contribution for the *R* case is close to zero, while for the *S* case, it is different from zero (4 kJ/mol). Because these interactions contribute to the total ΔE_{chir} with opposite signs, the resulting value of ΔE_{chir} is much smaller than the +6 kJ/mol value for the CO···CHO interaction. It should be noted that for both pairs, only one group is attached to the chiral center.

Finally, one should once again emphasize how misleading it could be looking for the strongest interactions if the goal is to identify the chiral-discriminating interactions. The carvone−CHO-menthol presents the excellent example to make such a distinction (see Figure 3xv) because the total chiral discrimination of 4 kJ/mol does not result from the two strongest interactions but from much weaker secondary interactions.

Summarizing, the replacement of the hydroxy group by the aldehyde group in menthol leads to the increase in chiral discrimination, which can be directly related to the interactions with the newly introduced functional group.

Carvone−NO_2-Menthol Complexes. Similarly, as in the previous case, the relative orientation of monomers in the carvone−NO_2-menthol complexes is not determined by the attraction of the carbonyl group and the substituent. Quite on the opposite, the distance between the oxygen from the −CO group and the closest atom of the nitro groups is equal to 4.99 Å

https://dx.doi.org/10.1021/acs.jpca.0c06266
J. Phys. Chem. A 2020, 124, 7735−7748

(N−O distance) and 5.30 Å (O−O distance) for the *S* and *R* cases, respectively. In both carvone−NO_2-menthol complexes, the major stabilization (of −19 and −22 kJ/mol for the *S* and *R* complexes, respectively) results from the interaction between MeM and the −CO group, which is predominantly of the electrostatic character (see Figure 3xvi,xvii). This fact is surprising, given a nonpolar character of the methyl group. Apparently, this group becomes polarized by the neighbor polar −CO group. The next most important interactions differ for the *S* and *R* cases. Although in the former case, it is the interaction of the carvone ring with the nitro group and the ring−ring interactions which contribute the most to the attraction between both molecules, for the latter case, only the ring−ring interaction is of similar importance, whereas the ring−NO_2 interaction is very small. A more detailed analysis reveals that the character of this interaction is different in both cases: although for the *S* case, the exchange contribution is small and does not attenuate a low electrostatic contribution (of −12 kJ/mol), for the *R* case, the electrostatic is small and repulsive and the exchange term cancels the large attraction coming from the dispersion component. Additionally, one can find two significant repulsive contributions to the total interaction energy, resulting from the interaction of −CO with the menthol ring and the menthol ring with MeC. It should be noted that the second from these interactions is of electrostatic character, which agrees with the postulate that the $-CH_3$ group has been polarized (see the analysis of the major stabilizing interaction).

The analysis of the chirally discriminating contributions (see Figure 3xviii) shows several unique features for the complexes with the NO_2−menthol. First of all, there are three ΔE_{chir} terms of a large absolute value between 17 and 7 kJ/mol, all resulting from the interaction with the substituent (NO_2). However, if only the first of these terms is taken into account, a wrong sign of the total ΔE_{chir} will be predicted. Similarly, the addition of the second and third most important terms does not heal the situation—actually, these three contributions sum to 0 kJ/mol, that is, not chiral discrimination. Only after the remaining contributions are included, the correct sign and order of magnitude of the ΔE_{chir} is recovered, among which one should mention the LC group and the menthol ring. Summarizing, the large ΔE_{chir} for this case shows that similarly to the CHO-menthol diastereoisomers, the elimination of the hydroxy group by a larger polar group can lead to the increased chiral discrimination.

Carvone−X-Menthol (Where X = F, Cl, and Br) Complexes. Next, three diastereoisomeric pairs are those resulting from the substitution of the −OH group in menthol by a halogen atom. The replacement of the hydrogen donor group by fluorine, chlorine, or bromine changes the dimer structure completely in comparison to complexes with the proper H-bond. In particular, the −CO group of carvone and chlorine or bromium atoms are placed on opposite sides of complexes, similarly to the CN-menthol and CHO-menthol cases. The oxygen−halogen distances are much longer than the O−O distance in the carvone−menthol complex: in the former case, the distances are longer than 5 Å (and even than 6 Å for one case), which should be compared with the 3 Å for the latter case. The fluorine-substituted case shows different relative orientations of the monomers in comparison to complexes with heavier halogen-menthol, but also in this case, the F−O distance amounts to about 4.5 Å (4.41 and 4.65 Å for the *S* or *R* case, respectively). (It should be parenthetically noted that the carvone−F-menthol conformers with geometries very similar to the heavier analogues represent local minima which are a couple of kJ/mol higher than the presented ones, and we have chosen to take into account the lowest energetically minima in our discussion.) The geometries of the complexes with two heavy halogens are especially similar for the pair (*R*)-carvone−Cl-menthol and (*R*)-carvone−Br-menthol, while another pair (*S*)-carvone−Cl-menthol and (*S*)-carvone−Br-menthol is a more different one from another.

Similarly to other cases where the highly polar −OH group serving as a hydrogen donor is absent and substituted by another group, no dominant group−group interaction can be identified, which is clearly seen from the graphs presented in Figure 3xix−xxvii. Quite the contrary, the total interaction energy is composed of several contributions of a comparable importance. For instance, for the fluorine case, two interactions contribute 15−25% to the total interaction energy, while for heavier analogues, there is between three and five such contributions.

The *S* and *R* diastereoisomers of the carvone−F-menthol complex differ in relative orientation of molecules, so it is quite surprising that these two species have virtually the same interaction energies and very small total $|\Delta E_{chir}|$. An analysis of graphs reveals that the carboxylic group of carvone plays an important role in the attractive part of the interaction energy in both cases; however, the F-menthol counterpart is different for the *S* and *R* complexes: it is the fluorine atom in the former case and the menthol ring in the latter. For the interaction between the −CO group and the menthol ring, the major difference between the *S* and *R* diastereoisomers is due to electrostatic and first-order exchange components which are known to be the most anisotropic, while induction and dispersion are quite similar to one another. Such a behavior is common for cases where interacting groups are in a similar distance from each other but differ in relative orientations. For the (*S*)-carvone−F-menthol, one can find a large attractive contribution between the −CO group and the fluorine atom, which has a purely electrostatic character and is equal to −10 kJ/mol. In contrast, the interaction for the (*R*)-carvone−F-menthol case is also purely electrostatic, but three times less attractive (−3.3 kJ/mol). Another important interaction is developed between the carvone ring and the LM group. Among three interaction pairs, those involving −CO show large differences between diastereoisomers (7 and −5 kJ/mol for −CO interacting with the fluorine atom and menthol ring, respectively). However, the inspection of the ΔE_{chir} graph shows that there are more significant differences in interactions between the *S* and *R* cases. For instance, the energy difference between the fluorine atom and the carvone ring amounts to −6 kJ/mol, which is due to the attractive electrostatic contribution for the (*R*)-carvone−F-menthol complex and virtually no interaction for the (*S*)-carvone−F-menthol one. A long-range dominant electrostatic contribution suggests a strong polarization of the fluorine atom in this case. A similar effect occurs for other halogen complexes with the exception of (*S*)-carvone−Cl-menthol. Therefore, the chiral discrimination in this case is close to zero because of the presence of the ΔE_{chir} terms of opposite signs and their accidental cancelation.

The most significant interaction for complexes with heavier halogen occurs between both rings for three out of four cases (with the exception of (*S*)-carvone−Br-menthol). Because of a large difference in the ring−ring interaction in complexes with bromine, this attraction contributes the most to the total ΔE_{chir} value (by −6 kJ/mol). For the (*S*)-carvone−Br-menthol case, the two most important interactions happen between the −CO

https://dx.doi.org/10.1021/acs.jpca.0c06266
J. Phys. Chem. A 2020, 124, 7735−7748

group and either the bromine atom or the menthol ring. The attraction within the latter pair is weaker by +4 kJ/mol for the *R* case, which indicates a partial cancellation of the ring−ring contribution to ΔE_{chir}. Similarly to the fluorine case, the interactions between the carboxylic group and −Cl or −Br are predominantly of electrostatic nature, which again indicates that the electron density of the halogen should be significantly polarized by the nearby groups. The strength of these interactions is similar to each other (between −7 and −8 kJ/mol) for both bromine-containing complexes and for (*R*)-carvone−Cl-menthol. For the remaining case, (*S*)-carvone−Cl-menthol, the Cl−O distance is 1.3 Å longer than that for for another diastereoisomer, and the partitioning shows virtually no interaction between the carboxylic group and the chlorine atom. This means that the ΔE_{chir} term between −Cl and −CO amounts to −7 kJ/mol and is one of the largest among group−group interactions. As already noted, it is not possible to identify a clearly dominant contribution for all these cases. Additionally, similarly to the complexes with F-menthol, a small total chiral discrimination for the bromine-containing complexes results from the accidental cancellation of otherwise large terms. For the interaction with the carvone ring, there are four different terms of a similar absolute value (4−5 kJ/mol), two with the plus and two with the minus sign, while for the −CO group, there are two such terms of opposite sign (with the menthol ring and the MeM group). It is also interesting to examine how differences in the placement of the electron-rich bromium atom influence the interaction strength and character of the interaction with the various types of carbon atoms of the carvone ring. In the (*S*)-carvone−Br-menthol complex, bromium is located above the carvone ring with the closest distance to the sp^2 carbon equal to 3.60 Å, resembling the orientation encountered for the nucleophilic substitution to the nearby double C═C bond. F-SAPT indicates that the energy of the interaction between −Br and the −CCH group (containing the abovementioned double bond) amounts to as much as −11 kJ/mol, out of which −7 kJ/mol is due to dispersion. A large contribution of dispersion can be expected for the electron-rich atom such as bromine. In the (*R*)-carvone−Br-menthol complex, bromium adapts a less favorable position, pointing at the saturated carbon from the ring (the distance equals 3.76 Å). The Br−C(sp^2) distance is similar (3.74 Å), but nonetheless, the Br···CCH interaction energy for the latter case is less attractive and equal to −8 kJ/mol with dispersion contributing to a half of this value.

The chlorine-menthol shows one of the largest ΔE_{chir} for the total interaction energy (−6 kJ/mol for F-SAPT and −3.6 kJ/mol for SAPT(DFT)); therefore, it is interesting to summarize here which groups contribute the most to this difference. F-SAPT partitioning shows that there are several binding interactions of a similar importance, from which the interaction between the menthol ring and the whole ring of carvone gives the major contribution (−13 and −12 kJ/mol for (*S*)-carvone−Cl-menthol and (*R*)-carvone−Cl-menthol, respectively). This interaction is largely of a dispersion character, especially for the latter case. Other important attractive contributions are the interactions of the chlorine atom with the double C═C bond and between methyl groups which are mostly electrostatic. However, none of these interactions contributes significantly to the chiral discrimination in these diastereoisomers. A more detailed analysis reveals that the most important in this aspect is the interaction of the carboxyl group of carvone and the chlorine atom. This electrostatic interaction is very weak for the (*S*)-carvone−Cl-menthol case (−1 kJ/mol only), while for the (*R*)-carvone−Cl-menthol complex, it amounts to as much as −8 kJ/mol. This difference can be explained by a larger separation of −Cl and −CO in the former case and a somewhat different orientation of the Cl−C and C−O bonds.

Finally, in view of a similar orientation of the *R*-carvone and the derivative of menthol for chlorine and bromine substituents, one is tempted to investigate the transferability of a partitioning of total interaction energies between pairs, as well as their SAPT components. Ideally, if the same orientation of carvone and the menthol derivative is preserved and the only change consists in changing the substituent, one would expect that only pairs in which the substituent takes part should be modified, while other pairs should exercise the same attraction and repulsion in both cases. A comparison of the partitioned contributions of F-SAPT for these two cases reveals that indeed differences between the energy components are very small for the terms where the substituent is not involved. For the vast majority of these components, the differences are less or equal to 0.1 kJ/mol. For electrostatic and dispersion interactions, the only differences above 1 kJ/mol are due to the interactions with chlorine or bromine, and for the first-order exchange, the two largest ones are also due to the pairs containing −Cl or −Br, while differences in induction contributions are smaller than 0.1 kJ/mol for all the cases. On the other hand, a similar comparison of the (*S*)-carvone−Cl-menthol and (*S*)-carvone−Br-menthol complexes reveals much larger differences between components of the interaction energies because of a different orientation of *S*-carvone and the derivative of menthol for almost all 16 interaction pairs.

Carvone−CN-Menthol Complexes. The next interesting derivative of menthol is the (1*R*,2*S*,5*R*)-2-isopropyl-5-methylcyclohexanecarbonitrile, denoted in the following as CN-menthol. The carvone−CN-menthol complexes show the highest chiral discrimination among the studied complexes, with the (*R*)-carvone−CN-menthol diastereoisomer being 4.8 kJ/mol more stable than the (*S*)-carvone−CN-menthol one, according to the saturated SAPT(DFT) results (see Table 2). As in many cases where the proper H-bonds cannot be formed, the substituent (carbonitrile) group is placed away from the −CO group of carvone. The distance between the closest atoms of these two groups is equal to 4.41 and 4.63 Å for the *S* and *R* complexes, respectively (in both cases, it is the distance between carbon atoms). The examination of the interaction graphs of the (*S*)-carvone−CN-menthol and (*R*)-carvone−CN-menthol (see Figure 3xxviii−xxx) reveals quite different distribution of attractive and repulsive components of the total interaction energy, leading to several large components of $|\Delta E_{chir}|$. Only for the former case, one can find a clearly dominating interaction, that is, the attraction between the carvone ring and the carbonitrile group. This interaction is quite strong (−20 kJ/mol) and has a predominantly electrostatic character, which is surprising because out of two interacting groups, only the carbonitrile one is polar. For the second diastereoisomer, the respective interaction energy is more than two times weaker—it amounts to −9 kJ/mol only. Therefore, already the first analyzed pair of functional groups gives a significant contribution to chiral discrimination. The second such pair is MeM and the carboxyl groups. This interaction is very weak (1 kJ/mol) for the (*R*)-carvone−CN-menthol complex and strongly attractive for the (*S*)-carvone−CN-menthol case (−14 kJ/mol), where it is also purely electrostatic. Therefore, this interaction is not only strong but also highly chirally discriminating, with the ΔE_{chir} = +15 kJ/mol. Surprisingly, from these two groups, only the MeM one is

https://dx.doi.org/10.1021/acs.jpca.0c06266
J. Phys. Chem. A 2020, 124, 7735−7748

attached to the chiral center, while the −CO group is separated from the chiral center by two bonds. It should be also noted that the sign of ΔE_{chir} for these two groups is opposite to the total ΔE_{chir}. From the remaining two interaction pairs, the CO···CN one is again predominantly electrostatic and attractive for one complex (this time, the (*R*)-carvone−CN-menthol one, with the energy equal to −10 kJ/mol) and almost zero for the second one. Therefore, the ΔE_{chir} value for this pair is equal to −9 kJ/mol. It should be noted that this time, the sign of this energy difference corresponds to the sign of the total difference from the table, and again only one group (−CN) is attached to the chiral center in spite of the large $|\Delta E_{chir}|$. The last strongly attractive interaction occurs between the menthol ring and the saturated part of the carvone ring (−9 and −8 kJ/mol).

The sum of the ΔE_{chir} terms from these interactions gives the wrong sign; therefore, again one should examine other group pairs. When the interaction energy differences are examined directly, one can find, apart from the CO···MeM and CO···CN, several other pairs with large absolute values of ΔE_{chir}. Among them, there is another pair involving the −CO group, the interaction with the menthol ring, with the ΔE_{chir} = −8 kJ/mol. The character of this interaction is of a mixed character with a significant dispersion component, which for the (*S*)-carvone−CN-menthol case is overcompensated by the strongly repulsive electrostatics. The carbonitrile group contributes to the remaining three significant difference energies: two attractive ones with MeC and LC (both −9 kJ/mol) and one repulsive—with the saturated part of the carvone ring (+9 kJ/mol). One should note that this time, the latter two pairs either contain the chiral center or are attached to it for both groups.

Summarizing, for the carvone−CN-menthol complexes, we have identified six chirally discriminating pairs, two with positive and four with negative ΔE_{chir}, giving altogether the strongest chiral discrimination for the whole test set of the derivatives of menthol.

Carvone−CH_3-Menthol Complexes. The substitution of the hydroxyl group with $-CH_3$ deprives the menthol from the only polar group, which takes part in a creation of the strong H-bond for the original carvone−menthol complexes. Nevertheless, the geometry optimization reveals that the lowest conformer for both *S* and *R* cases have the new methyl group placed close to the carboxyl group of carvone. Even the distance between the ring atom to which the substituent ($-CH_3$ or −OH) is attached and the carbon from the −CO group is similar for the substituted and unsubstituted cases (3.98 or 3.99 Å and 3.74 or 3.92 Å for the *S* and *R* complexes, respectively). However, the similarities between both cases end here. Other parts of CH_3-menthol are oriented quite differently in comparison to the carvone−menthol complexes, starting from the ring orientations.

Given the lack of the polar groups in both monomers, it is difficult to predict a priori the most important interactions between groups of these molecules. The examination of the interaction graphs (see Figure 3xxxi−xxxiii) reveals that there are six attractive contributions of a similar importance, which result from the interactions of the carvone ring or the menthol ring and the remaining (nonring) groups and one repulsive contribution between both rings. Interestingly, the latter contribution is composed of low dispersion interaction (−24 and −25 kJ/mol for the *S* and *R* cases, respectively), which is however damped with excess by the first-order exchange and small repulsive electrostatic contribution. The strongest attraction occurs between the carboxyl group and the menthol ring (−12 and −16 kJ/mol for (*S*)-carvone−CH_3-menthol and (*R*)-carvone−CH_3-menthol, respectively). At the same time, this interaction is among three most chiral discriminating ones in the present case. The interaction of the LC group and the menthol ring is of similar importance (−11 and −8 kJ/mol) and is also chiral-discriminating (ΔE_{chir} = +3 kJ/mol). The attraction between the carvone ring and the substituent ($-CH_3$) is also quite strong (−8 and −9 kJ/mol for the *S* and *R* complexes, respectively). Surprisingly, the partitioning of this energy into SAPT components shows the dominant contribution of electrostatics and the negligible first-order exchange. The lack of the exchange suggests a large distance between interacting fragments, which is confirmed by the geometry analysis, so the long-range electrostatics suggest a priori deformation of monomer densities in the regions of the carvone ring and the methyl group, which is large enough to allow for significant electrostatic contribution. Finally, the interaction of the $-CH_3$ group of carvone and the ring of menthol adds about −7 kJ/mol to the overall attraction, but in this case, there is no difference in interaction strength for both complexes.

Untypically, for the present case, the majority of the important interaction pairs also contribute significantly to the total ΔE_{chir}. The only group pair not listed so far is the substituent methyl group, which is electrostatically repelled by the carboxyl group for the (*R*)-carvone−CH_3-menthol case (+6 kJ/mol). The same interaction for the second diastereoisomer is much smaller so that the ΔE_{chir} for this pair amounts to 5 kJ/mol and is the largest among all group−group interactions. As in many previous cases, the absolute value of the total ΔE_{chir} is much smaller than the absolute values for individual group−group interactions.

CONCLUSIONS

In the present work, we studied the possibility of chiral discrimination of diastereoisomeric complexes composed of (*S*)- or (*R*)-carvone with (−)-menthol and its derivatives and tested to what extent the F-SAPT method can be applied to examine differences in interaction energies of these complexes (the so-called chirodiastaltic energy). In order to examine the substituent effect in detail, we have chosen to modify the menthol molecule by exchanging one group only (the hydroxy group) for the other functional group of varying character. At first, we examined differences in SAPT(DFT) interaction energies at the CBS limit for optimal structures for diastereoisomeric complexes containing (*S*)- or (*R*)-carvone and the same derivative of (−)-menthol, which turn out to be of the order of a few kJ/mol, with substituents increasing or decreasing this difference. The highest chirodiastaltic energy has been found for the −CN and $-NO_2$ substituents. On the other hand, the highest absolute value of the total interaction energy has been detected for the carvone−COOH-menthol complex, while the least attractive interaction occurs between carvone and CH_3-menthol, which also has the lowest value of chiral discrimination. These and other examples show that the large absolute value of the interaction energy and the value of chirodistaltic energy are not correlated with each other. The partition into SAPT components gives not enough information to answer the question which functional groups are the most important for the total interaction and for differences between diastereoisomers, but our studies show that this gap can be to a large extent filled with the F-SAPT method, for which the SAPT(HF) interaction energies and their components are partitioned into contributions belonging to the interaction of two functional groups. With this method, one can not only

https://dx.doi.org/10.1021/acs.jpca.0c06266
J. Phys. Chem. A 2020, 124, 7735−7748

detect H-bonds, which are characterized by a large contribution of electrostatics and net induction in the interaction energy between two groups, but also other interaction types, such as dispersion-dominated ring−ring interactions and so forth.

In this study, we have shown that also more subtle interaction *differences* are reproduced by the F-SAPT analysis of the interaction of diastereoisomeric complexes. It turns out that the overall small chirodiastaltic energies result from two different mechanisms: either differences in energies between *R* or *S* complexes are small for all interacting functional groups or individual differences are large in absolute magnitude for some pairs, but of opposite sign, resulting in a near cancellation of the total chiral effect. The first situation occurs for the $-NH_2$, $-COOH$, and $-CH_3$ substituents (individual difference contributions of at most a couple of kJ/mol), while the second one is especially pronounced (i.e., some individual contributions of 8 kJ/mol and higher) for $-NO_2$, $-CN$, and $-SH$ cases. The latter cases correspond to three out of four cases with the highest total $|\Delta E_{chir}|$, but still, this value is disappointingly small in comparison to individual differences for group−group interactions, which amount to 17 kJ/mol (carvone ring with $-NO_2$). For instance, for the carvone−CN-menthol complex, one identifies six important interactions between functional groups.

However, another aspect of our work was to verify the validity of the three-point rule, which states that the chiral differentiation of molecules is possible when there are at least three different intermolecular interactions between the interacting molecules (hydrogen-bond interactions, van der Waals bonds, dipole−dipole and charge-transfer types, and sterical repulsion) and if at least one of them is stereochemically dependent, that is, it depends on the chiral center of a given enantiomer. The examination of the obtained results shows that the identification of such interactions is often not sufficient for an effective chiral discrimination because of the cancellation of strong attractive and repulsive components. It also happens that the strongest chirally discriminating interactions belong to a pair of functional groups, which are not directly attached to a chiral center. This fact and the near cancellation of some contributions can be partially explained by the flexibility of the studied systems, which contain saturated bonds, and can adapt their geometries to a changing environment, significantly diminishing the effect of the chirally discriminating interaction. Therefore, the results for more rigid molecules would probably show a higher chiral discrimination. In the other case, one can say that the F-SAPT model has successfully passed one of the most difficult tests for a biologically important case, which is the carvone and menthol interaction.

Another application of F-SAPT is a demonstration of a transferability of interactions between functional groups, which remain the same in two pairs of diastereoisomeric complexes, provided that their relative positions in a new complex do not change considerably. In fact, for such situations (see e.g., halogen cases), the pair interactions remain quite similar to each other.

Summarizing, the F-SAPT model[4,5] proves to be a useful device for a detailed examination of intermolecular interactions, even for subtle interaction effects introduced by chirality. It gives us semiquantitative results which outperform the usually applied empirical rules, such as the three-point rule, which can be easily interpreted and compared, especially if graph visualization, as proposed in this study, is employed for this purpose.

■ ASSOCIATED CONTENT

Supporting Information

The Supporting Information is available free of charge at https://pubs.acs.org/doi/10.1021/acs.jpca.0c06266.

Figures of B97-D3/aug-cc-pVTZ optimized structures for the complexes under study; components of the SAPT(DFT)/aug-cc-pVDZ interaction energy for the complexes under study; components of the SAPT(DFT)/aug-cc-pVTZ interaction energy for the complexes under study; components of the SAPT(DFT)/aug-cc-pVQZ interaction energy for the complexes under study; components of the SAPT(DFT)/CBS interaction energy for the complexes under study; and interaction-strength graphs for complexes under studyComponents of the SAPT(MP)/aug-cc-pVDZ, SAPT(DFT)/aug-cc-pVnZ (n=D,T,Q), and SAPT(DFT)/CBS for the carvone - menthol complexes; figures of the B97-D3/aug-cc-pVTZ optimised structures for the complexes under study; and interaction-strength graphs for the complexes under study (PDF)

Cartesian coordinates of the complexes under study (XYZ)

■ AUTHOR INFORMATION

Corresponding Author

Tatiana Korona − *Faculty of Chemistry, University of Warsaw, 02-093 Warsaw, Poland;* orcid.org/0000-0001-7169-3412; Email: tania@chem.uw.edu.pl

Authors

Michał Chojecki − *Faculty of Chemistry, University of Warsaw, 02-093 Warsaw, Poland;* orcid.org/0000-0002-4590-5845

Dorota Rutkowska-Zbik − *Jerzy Haber Institute of Catalysis and Surface Chemistry, Polish Academy of Sciences, 30-239 Cracow, Poland;* orcid.org/0000-0001-9323-1710

Complete contact information is available at: https://pubs.acs.org/10.1021/acs.jpca.0c06266

Notes

The authors declare no competing financial interest.

■ ACKNOWLEDGMENTS

The support from the National Science Centre of Poland through grant 2015/19/B/ST4/01812 is gratefully acknowledged. This research was supported in part by PL-Grid Infrastructure.

■ REFERENCES

(1) Jeziorski, B.; Moszynski, R.; Szalewicz, K. Perturbation Theory Approach to Intermolecular Potential Energy Surfaces of van der Waals Complexes. *Chem. Rev.* **1994**, *94*, 1887−1930.

(2) Szalewicz, K. Symmetry-Adapted Perturbation Theory of Intermolecular Forces. *Wiley Interdiscip. Rev. Comput. Mol. Sci.* **2012**, *2*, 254−272.

(3) Patkowski, K. Recent Developments in Symmetry-Adapted Perturbation Theory. *Wiley Interdiscip. Rev. Comput. Mol. Sci.* **2020**, *10*, No. e1452.

(4) Parrish, R. M.; Sherrill, C. D. Spatial Assignment of Symmetry Adapted Perturbation Theory Interaction Energy Components: the Atomic SAPT Partition. *J. Chem. Phys.* **2014**, *141*, 044115.

(5) Parrish, R. M.; Parker, T. M.; Sherrill, C. D. Chemical Assignment of Symmetry-Adapted Perturbation Theory Interaction Energy

Components: The Functional-Group SAPT Partition. *J. Chem. Theory Comput.* **2014**, *10*, 4417−4431.
(6) Parrish, R. M.; Sitkoff, D. F.; Cheney, D. L.; Sherrill, C. D. The Surprising Importance of Peptide Bond Contacts in Drug-Protein Interactions. *Chem.—Eur. J.* **2017**, *23*, 7887−7890.
(7) Chojecki, M.; Rutkowska-Zbik, D.; Korona, T. On the Applicability of Functional-Group Symmetry-Adapted Perturbation Theory and Other Partitioning Models for Chiral Recognition - the Case of Popular Drug Molecules Interacting with Chiral Phases. *Phys. Chem. Chem. Phys.* **2019**, *21*, 22491−22510.
(8) Chojecki, M.; Rutkowska-Zbik, D.; Korona, T. Dimerization Behavior of Methyl Chlorophyllide a as the Model of Chlorophyll a in the Presence of Water Molecules - Theoretical Study. *J. Chem. Inf. Model.* **2019**, *59*, 2123−2140.
(9) Hemmati, R.; Patkowski, K. Chiral Self Recognition: Interactions in Propylene Oxide Complexes. *J. Phys. Chem. A* **2019**, *123*, 8607−8618.
(10) Oertling, H.; Reckziegel, A.; Surburg, H.; Bertram, H.-J. Applications of Menthol in Synthetic Chemistry. *Chem. Rev.* **2007**, *107*, 2136−2164.
(11) Hawrył, M. A.; Skalicka-Woźniak, K.; Świeboda, R.; Niemiec, M.; Stępak, K.; Waksmundzka-Hajnos, M.; Hawrył, A.; Szymczak, G. GC-MS Fingerprints of Mint Essential Oils. *Open Chem.* **2015**, *13*, 1326−1332.
(12) Nandi, N. Molecular Origin of the Recognition of Chiral Odorant by Chiral Lipid: Interaction of Dipalmitoyl Phosphatidyl Choline and Carvone. *J. Phys. Chem. A* **2003**, *107*, 4588−4591.
(13) Geithe, C.; Protze, J.; Kreuchwig, F.; Krause, G.; Krautwurst, D. Structural Determinants of a Conserved Enantiomer-Selective Carvone Binding Pocket in the Human Odorant Receptor OR1A1. *Cell. Mol. Life Sci.* **2017**, *74*, 4209−4229.
(14) Gries, K.; Bubel, K.; Wohlfahrt, M.; Agarwal, S.; Koert, U.; Greiner, A. Preparation of Gold Nanoparticle- Poly(L-menthyl methacrylate) Conjugates via ATRP Polymerization. *Macromol. Chem. Phys.* **2011**, *212*, 2551−2557.
(15) Yingngam, B.; Chiangsom, A.; Pharikarn, P.; Vonganakasame, K.; Kanoknitthiran, V.; Rungseevijitprapa, W.; Prasitpuriprecha, C. Optimization of Menthol-Loaded Nanocapsules for Skin Application Using the Response Surface Methodology. *J. Drug Delivery Sci. Technol.* **2019**, *53*, 101138.
(16) Chastrette, M.; Rallet, E. Structure-Minty Odour Relationships: Suggestion of an Interaction Pattern. *Flavour Fragrance J.* **1998**, *13*, 5−18.
(17) Kamatou, G. P. P.; Vermaak, I.; Viljoen, A. M.; Lawrence, B. M. Menthol: A Simple Monoterpene with Remarkable Biological Properties. *Phytochemistry* **2013**, *96*, 15−25.
(18) Wilbon, P. A.; Chu, F.; Tang, C. Progress in Renewable Polymers from Natural Terpenes, Terpenoids, and Rosin. *Macromol. Rapid Commun.* **2013**, *34*, 8−37.
(19) Vishwakarma, S.; Kumari, A.; Mitra, K.; Singh, S.; Singh, R.; Singh, J.; Sen Gupta, S. K.; Ray, B. L-Menthol-Based Initiators for Atom Transfer Radical Polymerization of Styrene. *J. Appl. Polym. Sci.* **2019**, *136*, 47964.
(20) Lowe, J. R.; Martello, M. T.; Tolman, W. B.; Hillmyer, M. A. Functional Biorenewable Polyesters from Carvone-Derived Lactones. *Polym. Chem.* **2011**, *2*, 702−708.
(21) Oubella, A.; Ait Itto, M. Y.; Auhmani, A.; Riahi, A.; Robert, A.; Daran, J.-C.; Morjani, H.; Parish, C. A.; Esseffar, M. h. Diastereoselective Synthesis and Cytotoxic Evaluation of new Isoxazoles and Pyrazoles with Monoterpenic Skeleton. *J. Mol. Struct.* **2019**, *1198*, 126924.
(22) Xu, B.; Wang, B.; Xun, W.; Qiu, F. G. Total Synthesis of (−)-Daphenylline. *Angew. Chem., Int. Ed.* **2019**, *58*, 5754−5757.
(23) McCann, J. L.; Rauk, A.; Wieser, H. A Conformational Study of (1S, 2R, 5S)-(+)-Menthol Using Vibrational Circular Dichroism Spectroscopy. *Can. J. Chem.* **1998**, *76*, 274−283.
(24) Hoffmann, G. G. Infrared, Raman and VCD Spectra of (S)-(+)-Carvone-Comparison of Experimental and ab initio Theoretical Results. *J. Mol. Struct.* **2003**, *661−662*, 525−539.
(25) Avilés Moreno, J. R.; Partal Ureña, F.; López González, J. J. Conformational Landscape in Chiral Terpenes from Vibrational Spectroscopy and Quantum Chemical Calculations: S-(+)-Carvone. *Vib. Spectrosc.* **2009**, *51*, 318−325.
(26) Shen, J.; Li, Y.; Vaz, R.; Izumi, H. Revisiting Vibrational Circular Dichroism Spectra of (S)-(+)-Carvone and (1S,2R,5S)-(+)-Menthol Using SimIR/VCD Method. *J. Chem. Theory Comput.* **2012**, *8*, 2762−2768.
(27) Egawa, T.; Kachi, Y.; Takeshima, T.; Takeuchi, H.; Konaka, S. Structural Determination of Carvone, a Component of Spearmint, by means of Gas Electron Diffraction Augmented by Theoretical Calculations. *J. Mol. Struct.* **2003**, *658*, 241−251.
(28) Lambert, J.; Compton, R. N.; Crawford, T. D. The Optical Activity of Carvone: A Theoretical and Experimental Investigation. *J. Chem. Phys.* **2012**, *136*, 114512.
(29) Coriani, S.; Pecul, M.; Rizzo, A.; Jørgensen, P.; Jaszuński, M. Ab initio Study of Magnetochiral Birefringence. *J. Chem. Phys.* **2002**, *117*, 6417−6428.
(30) Jansík, B.; Rizzo, A.; Frediani, L.; Ruud, K.; Coriani, S. Combined Density Functional/Polarizable Continuum Model Study of Magneto-chiral Birefringence: Can Theory and Experiment be Brought to Agreement? *J. Chem. Phys.* **2006**, *125*, 234105.
(31) Zeroual, A.; Ríos-Gutiérrez, M.; Amiri, O.; El Idrissi, M.; Domingo, L. R. A Molecular Electron Density Theory Study of the Mechanism, Chemo- and Stereoselectivity of the Epoxidation Reaction of R-Carvone with Eeracetic Acid. *RSC Adv.* **2019**, *9*, 28500−28509.
(32) Pathirana, S.; Neely, W. C.; Myers, L. J.; Vodyanoy, V. Chiral Recognition of Odorants (+)- and (-)-Carvone by Phospholipid Monolayers. *J. Am. Chem. Soc.* **1992**, *114*, 1404−1405.
(33) Thirumoorthy, K.; Nandi, N. Comparison of the Intermolecular Energy Surfaces of Amino Acids: Orientation-Dependent Chiral Discrimination. *J. Phys. Chem. B* **2006**, *110*, 8840−8849.
(34) O'Boyle, N. M.; Banck, M.; James, C. A.; Morley, C.; Vandermeersch, T.; Hutchison, G. R. Open Babel: An Open Chemical Toolbox. *J. Cheminf.* **2011**, *3*, 33.
(35) Trott, O.; Olson, A. J. AutoDock Vina: Improving the Speed and Accuracy of Docking with a New Scoring Function, Efficient Optimization, and Multithreading. *J. Comput. Chem.* **2010**, *31*, 455−461.
(36) Grimme, S. Semiempirical GGA-Type Density Functional Constructed with a Long-Range Dispersion Correction. *J. Comput. Chem.* **2006**, *27*, 1787−1799.
(37) Dunning, T. H. Gaussian Basis Sets for Use in Correlated Molecular Calculations. I. The Atoms Boron through Neon and Hydrogen. *J. Chem. Phys.* **1989**, *90*, 1007−1023.
(38) Kendall, R. A.; Früchtl, H. A. The Impact of the Resolution of the Identity Approximate Integral Method on Modern ab initio Algorithm Development. *Theor. Chem. Acc.* **1997**, *97*, 158−163.
(39) Weigend, F.; Köhn, A.; Hättig, C. Efficient Use of the Correlation Consistent Basis Sets in Resolution of the Identity MP2 Calculations. *J. Chem. Phys.* **2002**, *116*, 3175−3183.
(40) *TURBOMOLE V7.3*, 2018, a development of University of Karlsruhe and Forschungszentrum Karlsruhe GmbH, 1989-2007; TURBOMOLE GmbH, since 2007; available from http://www.turbomole.com.
(41) Misquitta, A. J.; Szalewicz, K. Intermolecular Forces from Asymptotically Corrected Density Functional Description of Monomers. *Chem. Phys. Lett.* **2002**, *357*, 301−306.
(42) Heßelmann, A.; Jansen, G. First-Order Intermolecular Interaction Energies from Kohn-Sham Orbitals. *Chem. Phys. Lett.* **2002**, *357*, 464−470.
(43) Heßelmann, A.; Jansen, G.; Schütz, M. Density-Functional Theory-Symmetry-Adapted Intermolecular Perturbation Theory with Density Fitting: A New Efficient Method to Study Intermolecular Interaction Energies. *J. Chem. Phys.* **2005**, *122*, 014103.
(44) Perdew, J. P.; Burke, K.; Ernzerhof, M. Generalized Gradient Approximation Made Simple. *Phys. Rev. Lett.* **1996**, *77*, 3865−3868.

https://dx.doi.org/10.1021/acs.jpca.0c06266
J. Phys. Chem. A 2020, 124, 7735−7748

(45) Adamo, C.; Barone, V. Toward Reliable Density Functional Methods without Adjustable Parameters: The PBE0 Model. *J. Chem. Phys.* **1999**, *110*, 6158−6170.
(46) Grüning, M.; Gritsenko, O. V.; van Gisbergen, S. J. A.; Baerends, E. J. Shape Corrections to Exchange-Correlation Potentials by Gradient-Regulated Seamless Connection of Model Potentials for Inner and Outer Region. *J. Chem. Phys.* **2001**, *114*, 652−660.
(47) Korona, T. A Coupled Cluster Treatment of Intramonomer Electron Correlation Within Symmetry-Adapted PerturbationTtheory: Benchmark Calculations and a Comparison with a Density-Functional Theory description. *Mol. Phys.* **2013**, *111*, 3705−3715.
(48) Helgaker, T.; Klopper, W.; Koch, H.; Noga, J. Basis-Set Convergence of Correlated Calculations on Water. *J. Chem. Phys.* **1997**, *106*, 9639−9646.
(49) Werner, H.-J.; Knowles, P. J.; Knizia, G.; Manby, F. R.; Schütz, M.; Celani, P.; Györffy, W.; Kats, D.; Korona, T.; Lindh, R.; et al. *MOLPRO*, version 2015.1, a package of ab initio programs, 2015; see http://www.molpro.net.
(50) Werner, H.-J.; Knowles, P. J.; Manby, F. R.; Black, J. A.; Doll, K.; Heßelmann, A.; Kats, D.; Köhn, A.; Korona, T.; Kreplin, D. A.; et al. The Molpro Quantum Chemistry Package. *J. Chem. Phys.* **2020**, *152*, 144107.
(51) Szalewicz, K.; Patkowski, K.; Jeziorski, B. Intermolecular Interactions via Perturbation Theory: From Diatoms to Biomolecules. *Struct. Bond.* **2005**, *116*, 43−117.
(52) Moszynski, R.; Heijmen, T. G. A.; Jeziorski, B. Symmetry-Adapted Perturbation Theory for the Calculation of Hartree-Fock Interaction Energies. *Mol. Phys.* **1996**, *88*, 741−758.
(53) Hohenstein, E. G.; Sherrill, C. D. Density Fitting and Cholesky Decomposition Approximations in Symmetry-Adapted Perturbation Theory: Implementation and Application to Probe the Nature of $\pi - \pi$ Interactions in Linear Acenes. *J. Chem. Phys.* **2010**, *132*, 184111.
(54) Hohenstein, E. G.; Sherrill, C. D. Density Fitting of Intramonomer Correlation Effects in Symmetry-Adapted Perturbation Theory. *J. Chem. Phys.* **2010**, *133*, 014101.
(55) Hohenstein, E. G.; Parrish, R. M.; Sherrill, C. D.; Turney, J. M.; Schaefer, H. F. Large-Scale Symmetry-Adapted Perturbation Theory Computations via Density Fitting and Laplace Transformation Techniques: Investigating the Fundamental Forces of DNA-Intercalator Interactions. *J. Chem. Phys.* **2011**, *135*, 174107.
(56) Hohenstein, E. G.; Sherrill, C. D. Wavefunction Methods for Noncovalent Interactions. *Wiley Interdiscip. Rev. Comput. Mol. Sci.* **2012**, *2*, 304−326.
(57) Parrish, R. M.; Hohenstein, E. G.; Sherrill, C. D. Tractability Gains in Symmetry-Adapted Perturbation Theory Including Coupled Double Excitations: CCD+ST(CCD) Dispersion with Natural Orbital Truncations. *J. Chem. Phys.* **2013**, *139*, 174102.
(58) Parker, T. M.; Burns, L. A.; Parrish, R. M.; Ryno, A. G.; Sherrill, C. D. Levels of Symmetry Adapted Perturbation Theory (SAPT). I. Efficiency and Performance for Interaction Energies. *J. Chem. Phys.* **2014**, *140*, 094106.
(59) Parrish, R. M.; Burns, L. A.; Smith, D. G. A.; Simmonett, A. C.; DePrince, A. E.; Hohenstein, E. G.; Bozkaya, U.; Sokolov, A. Y.; Di Remigio, R.; Richard, R. M.; et al. Psi4 1.1: An Open-Source Electronic Structure Program Emphasizing Automation, Advanced Libraries, and Interoperability. *J. Chem. Theory Comput.* **2017**, *13*, 3185−3197.
(60) Papajak, E.; Zheng, J.; Xu, X.; Leverentz, H. R.; Truhlar, D. G. Perspectives on Basis Sets Beautiful: Seasonal Plantings of Diffuse Basis Functions. *J. Chem. Theory Comput.* **2011**, *7*, 3027−3034.
(61) Portmann, S.; Inauen, A.; Lüthi, H. P.; Leutwyler, S. Chiral Discrimination in Hydrogen-Bonded Complexes. *J. Chem. Phys.* **2000**, *113*, 9577−9585.
(62) Moszyński, R.; Rybak, S.; Cybulski, S.; Chałasiński, G. Correlation Correction to the Hartree-Fock Electrostatic Energy Including Orbital Relaxation. *Chem. Phys. Lett.* **1990**, *166*, 609−614.
(63) Moszynski, R.; Jeziorski, B.; Szalewicz, K. Many-body Theory of Exchange Effects in Intermolecular Interactions. Second-Quantization Approach and Comparison with Full Configuration Interaction Results. *J. Chem. Phys.* **1994**, *100*, 1312−1325.
(64) Moszyński, R.; Cybulski, S. M.; Chaasiński, G. Many-Body Theory of Intermolecular Induction Interactions. *J. Chem. Phys.* **1994**, *100*, 4998−5010.
(65) Moszynski, R.; Jeziorski, B.; Rybak, S.; Szalewicz, K.; Williams, H. L. Many-Body Theory of Exchange Effects in Intermolecular Interactions. Density Matrix Approach and Applications to He-F^-, He-HF, H_2-HF, and Ar-H_2 dimers. *J. Chem. Phys.* **1994**, *100*, 5080−5092.
(66) Moszynski, R.; Jeziorski, B.; Ratkiewicz, A.; Rybak, S. a. Many-Body Perturbation Theory of Electrostatic Interactions Between Molecules: Comparison with Full Configuration Interaction for Four-Electron Dimers. *J. Chem. Phys.* **1993**, *99*, 8856−8869.
(67) Korona, T. Second-Order Exchange-Induction Energy of Intermolecular Interactions from Coupled Cluster Density Matrices and their Cumulants. *Phys. Chem. Chem. Phys.* **2008**, *10*, 6509.
(68) Řezáč, J.; Hobza, P. Extrapolation and Scaling of the DFT-SAPT Interaction Energies toward the Basis Set Limit. *J. Chem. Theory Comput.* **2011**, *7*, 685−689.
(69) Günter Kindel, F. O. Use of Certain Isopropylmethylcyclohexenthiols as Odorous and/or Aroma Substances. EP 2266421 A1, 2010. https://lens.org/127-430-618-956-14X.

https://dx.doi.org/10.1021/acs.jpca.0c06266
J. Phys. Chem. A 2020, 124, 7735−7748